

# Effect of $Zn^{2+}$ concentration on the microstructure and magnetic properties of nanocrystalline $Co_{1-x}Zn_xFe_2O_4$ ferrites powder

LIU YIN\*, ZHANG LEI, GAN ZHI-PING<sup>a</sup>, MA LI-YUN<sup>a</sup>, MIN FAN-FEI, ZHANG MING-XU

*School of Materials Science and Engineering, Anhui University of Science and Technology, Huainan 232001, Anhui, China*

*<sup>a</sup>China Triumph International Engineering Group Co. Ltd, Bengbu 233018, Anhui, China*

Nanocrystalline  $Co_{1-x}Zn_xFe_2O_4$  ferrites powder were prepared by the spraying-coprecipitation method. Their microstructure and magnetic properties were investigated by XRD, TEM as well as VSM. The results show that nanocrystalline  $Co_{1-x}Zn_xFe_2O_4$  ferrites powder are spinel phase. The average crystallite size of nanocrystalline  $Co_{1-x}Zn_xFe_2O_4$  ferrites powder calcined at 700 °C for 1.5 h is about 32 nm. The lattice parameter  $a$  of nanocrystalline  $Co_{1-x}Zn_xFe_2O_4$  ferrites powder increases with the  $Zn^{2+}$  ions concentration. The enhancement of the magnetization up to maximum value of  $83.4 A \cdot m^2 \cdot kg^{-1}$  in nanocrystalline  $Co_{0.7}Zn_{0.3}Fe_2O_4$  ferrite powder is observed. This can be attributed to the change of the net magnetic moment between the sublattices for the substitution of the  $Co^{2+}$  ions with  $Zn^{2+}$  ions. The coercivity  $H_c$  of nanocrystalline  $Co_{1-x}Zn_xFe_2O_4$  ferrites powder decreases with  $Zn^{2+}$  ions concentration.

(Received April 13, 2012; accepted July 19, 2012)

**Keywords:** Nanocrystalline materials,  $Co_{1-x}Zn_xFe_2O_4$  ferrite, Microstructure, Magnetic properties

## 1. Introduction

The magnetic properties of nanoparticles have been of great interest in recent years, partly because the nanosize constituent particles or crystallites could be used as the high-density magnetic storage media [1, 2]. Much attention has been paid to the investigation of nanophase spinel ferrite particles. This is due to their technological importance in the application areas of microwave devices, high speed digital tape and disk recordings, magnetofluids, catalysis, and magnetic refrigeration systems [3].

Cobalt ferrite ( $CoFe_2O_4$ ) is a typical hard magnetic material. It has been commercialized in applications of recording media material due to the suitable coercivity ( $H_c$ ), the saturation magnetization ( $\sigma_s$ ) and strong anisotropy [4]. The cobalt ferrite is also known as a magneto-optical material, which shows an interesting light-induced coercivity change [5]. It had been shown that the microstructure and properties of  $CoFe_2O_4$  could be modified by the addition of metal cations, such as  $Ni^{2+}$ ,  $Zn^{2+}$ ,  $Mn^{2+}$  and rare earth cation [6-11]. In this paper, nanocrystalline  $Co_{1-x}Zn_xFe_2O_4$  ferrites powder were synthesized by the spraying-coprecipitation method. The effect of  $Zn^{2+}$  concentration on their microstructure and magnetic properties were investigated.

## 2. Experimental

The preparation of the nanocrystalline  $Co_{1-x}Zn_xFe_2O_4$  ferrites powder with the variable  $x$  ( $x = 0, 0.3, 0.5$  and  $0.7$ ) was accomplished by using the modified coprecipitation method (spraying coprecipitation synthesis process) [12]. Firstly, reagent-grade chemicals, including zinc chloride, cobalt sulphate and iron chloride (Sinopharm Chemical Reagent Co., Ltd.), were initially dissolved in a jar. The variable  $x$  was controlled by the ratios of used chemicals. This was followed by the titration of the sodium-hydroxide solution being sprayed into the flask assisted by the pressurized nitrogen as a carrying gas. The mixture was stirred to obtain the precipitates, which were washed several times using distilled water. The precursors were obtained and dried at about 100 °C for 24 h, and calcined at different temperatures to form the  $Co_{1-x}Zn_xFe_2O_4$  ferrites.

The crystalline structure of nanocrystalline  $Co_{1-x}Zn_xFe_2O_4$  ferrites powder was examined by the X-ray diffraction (XRD) spectrometer (Shimadzu LabX XRD-6000) using  $Cu-K\alpha$  radiation. Its microstructure was observed through the transmission electron microscope (TEM, JEM-200CX). The specific surface area of the sample was determined by the Brunauer-Emmett-Teller (BET) method with nitrogen adsorption. The magnetization measurements of samples were performed using the vibrating sample magnetometer (VSM, LakeShore7307-9309) under an external field between -10

and 10 kOe at room temperature.

### 3. Results

#### 3.1. Crystal structure and grain size

Fig. 1 shows the XRD patterns of Co<sub>1-x</sub>Zn<sub>x</sub>Fe<sub>2</sub>O<sub>4</sub> ferrites powder calcined at 700 °C for 1.5 h. It can be seen that all diffraction peaks are identified to be a spinel crystalline structure. No other phase is detected on these samples. The average crystallite size  $d$  of the powder can be obtained by the Scherrer formula:

$$d = 0.9 \cdot \lambda / (\beta \cdot \cos \theta) \quad (1)$$

Where  $\lambda$  is the X ray wavelength,  $\beta$  is the full width at half-maximum and  $\theta$  is the Bragg angle corresponding to the diffraction peak. Mean crystallite size of Co<sub>1-x</sub>Zn<sub>x</sub>Fe<sub>2</sub>O<sub>4</sub> ferrites powder is around 32 nm.

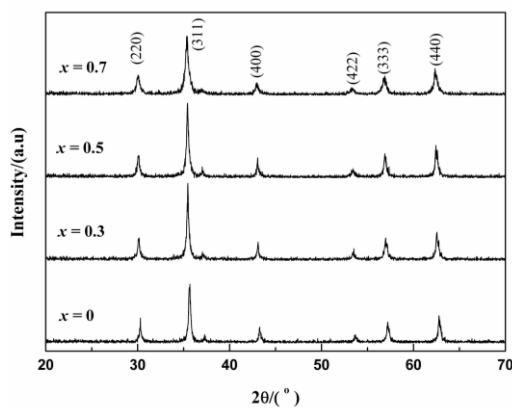


Fig. 1. XRD patterns of nanocrystalline Co<sub>1-x</sub>Zn<sub>x</sub>Fe<sub>2</sub>O<sub>4</sub> ferrites powder calcined at 700 °C for 1.5 h.

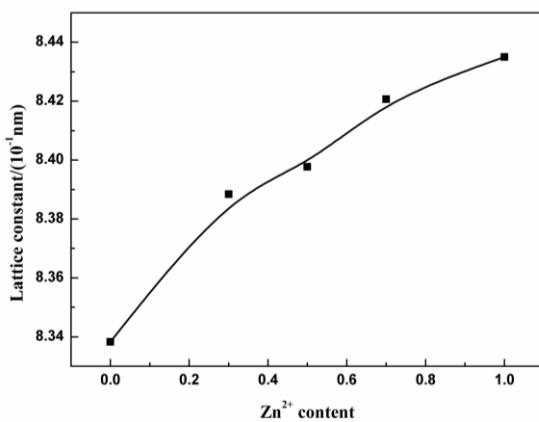


Fig. 2. Lattice constant of nanocrystalline Co<sub>1-x</sub>Zn<sub>x</sub>Fe<sub>2</sub>O<sub>4</sub> ferrites powder.

The Lattice constant  $a$  of nanocrystalline Co<sub>1-x</sub>Zn<sub>x</sub>Fe<sub>2</sub>O<sub>4</sub> ferrites powder with different Zn<sup>2+</sup> ions concentrations are calculated by formula as follow:

$$a = \frac{\lambda \cdot \sqrt{h^2 + k^2 + l^2}}{2 \cdot \sin \theta} \quad (2)$$

Where  $a$  is lattice parameter,  $\lambda$  is wavelength of Cu K $\alpha$  radiation, and  $h, k, l$  are indices of crystallographic plane. Fig. 2 shows lattice parameter ( $a$ ) linearly increase with the increase of Zn<sup>2+</sup> ions concentration in Co<sub>1-x</sub>Zn<sub>x</sub>Fe<sub>2</sub>O<sub>4</sub> ferrites. It increases from 8.338 Å to 8.421 Å as the range of Zn<sup>2+</sup> ions concentration increases from 0 to 0.7. This trend ascribed that the radius of Zn<sup>2+</sup> ions (0.74 Å) is larger than that of Co<sup>2+</sup> ions (0.65 Å). The substitution by larger ions results in expansion of crystal lattice of Co<sub>1-x</sub>Zn<sub>x</sub>Fe<sub>2</sub>O<sub>4</sub> ferrites. Therefore, an increase in the value of lattice parameter  $a$  is expected when Co<sup>2+</sup> ions is replaced by Zn<sup>2+</sup> ions.

#### 3.2. Microstructure

Fig. 3 shows a typical TEM image of the sample calcined at the temperature of 700 °C for 1.5 h. One can see that the average crystallite size of sample is around 50 nm, which is consistent with XRD pattern analysis results. A few of large agglomerate particle are seen in Fig. 3. It is ascribed to the intense surface effect of nanosized materials in order to minimize its magnetostatic energy and surface energy.

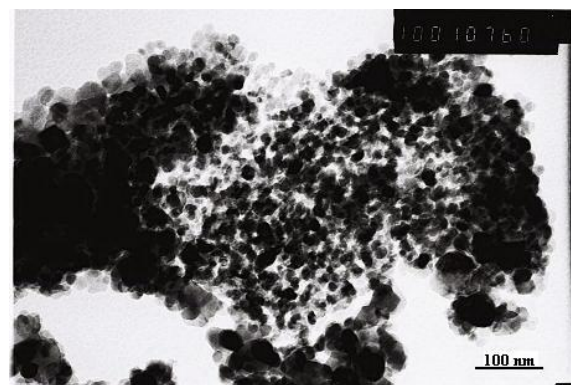


Fig. 3. TEM of nanocrystalline Co<sub>1-x</sub>Zn<sub>x</sub>Fe<sub>2</sub>O<sub>4</sub> ferrites powder calcined at 700 °C for 1.5 h.

#### 3.3. Magnetic properties

Fig. 4 shows hysteresis loops of nanocrystalline Co<sub>1-x</sub>Zn<sub>x</sub>Fe<sub>2</sub>O<sub>4</sub> ferrites powder at room temperature. All samples show hysteresis, its magnetization reached saturation at the external field of 800 kA·m<sup>-1</sup>. The

variation of specific saturation magnetization  $\sigma_s$  and coercivity  $H_c$  of nanocrystalline  $\text{Co}_{1-x}\text{Zn}_x\text{Fe}_2\text{O}_4$  ferrites powder is shown in Fig. 5. It can be seen that the specific saturation magnetization  $\sigma_s$  of samples increased with the concentration of Zinc ion at room temperature. The maximum of  $\sigma_s$  was about  $83.4 \text{ A}\cdot\text{m}^2\cdot\text{kg}^{-1}$  as the concentration of zinc ion was 0.3. Corresponding to this change, the coercivity  $H_c$  of samples decreased with the zinc ion concentration.

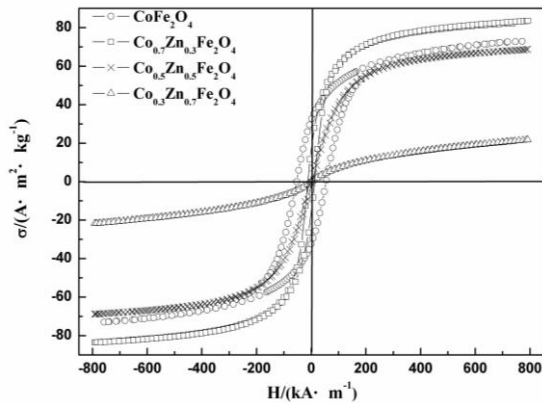


Fig. 4. Hysteresis loops of nanocrystalline  $\text{Co}_{1-x}\text{Zn}_x\text{Fe}_2\text{O}_4$  ferrites powder.

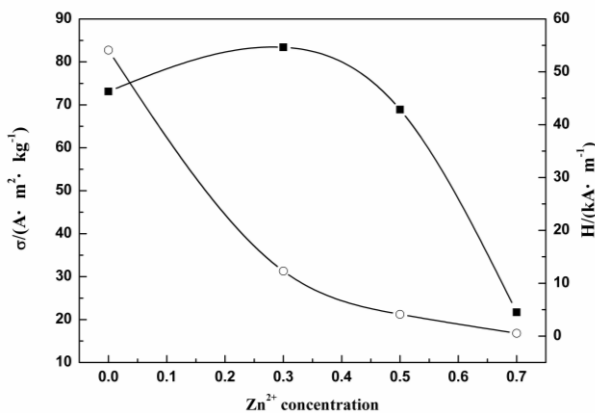


Fig. 5. Magnetic properties of nanocrystalline  $\text{Co}_{1-x}\text{Zn}_x\text{Fe}_2\text{O}_4$  ferrites powder.

#### 4. Discussion

A general chemical formula of the spinel ferrite could be presented as  $(\text{M}_\delta\text{Fe}_{1-\delta})[\text{M}_{1-\delta}\text{Fe}_{1+\delta}]\text{O}_4$ , where the cations in the parentheses occupied tetrahedral sites (A), and the cations in the square bracket occupied octahedral sites [B]. The overall net magnetic moment  $M$  of spinel-type ferrite was equal to  $M_B - M_A$  [13]. The cationic distribution in the spinel ferrite was mainly dependent on the radius of ions and their crystal energy, etc. The preference potentials of cations occupying tetrahedral A-site in the spinel ferrite were presented as [14]:

$$\text{Zn}^{2+} > \text{Mn}^{2+} > \text{Fe}^{3+} > \text{Fe}^{2+} > \text{Co}^{2+} > \text{Mn}^{3+} > \text{Ni}^{2+}$$

Zinc ions ( $\text{Zn}^{2+}$ ) preferred to occupy the tetrahedral A-site in the nanocrystalline  $\text{Co}_{1-x}\text{Zn}_x\text{Fe}_2\text{O}_4$  ferrite. The magnetic moment  $\mu$  per ion for  $\text{Zn}^{2+}$ ,  $\text{Fe}^{3+}$  and  $\text{Co}^{2+}$  ions are  $0 \mu_B$ ,  $5 \mu_B$  and  $3 \mu_B$  [15], respectively.

With the substitution of  $\text{Co}^{2+}$  ions by  $\text{Zn}^{2+}$  ions to make  $\text{Co}_{1-x}\text{Zn}_x\text{Fe}_2\text{O}_4$  ferrites, the  $\text{Zn}^{2+}$  ions mainly occupy tetrahedral sites (A) in spinel ferrite [16]. This leads to a restructuring of  $(\text{Zn}_x\text{Fe}_{1-x})[\text{Co}_{1-x}\text{Fe}_{1+x}]\text{O}_4$  ferrite. As a consequence, the cationic distribution causes two opposite effects in the net magnetic moment of the unit cell. On the one hand, the zinc ions decrease the magnetic moment of the sublattice A, but the  $\text{Co}^{2+}$  ions into octahedral sites (B) increase the magnetic moment of the sublattice B. Thus the net magnetic moment  $M$  of  $\text{Co}_{1-x}\text{Zn}_x\text{Fe}_2\text{O}_4$  ferrite is increased with  $\text{Zn}^{2+}$  ion concentration. On the other hand, a change in the  $\text{Zn}^{2+}$  ions concentration reduces the number of  $\text{Fe}^{3+}$  ions at the A sites, reducing the magnitude of superexchange coupling between the sublattices A and B, which tends to reduce the magnetic moment. It has been proved in Ref. [13] that the former is present at low  $\text{Zn}^{2+}$  ions concentration, while the latter becomes more important at high  $\text{Zn}^{2+}$  ions concentration. So maximum specific saturation magnetization  $\sigma_s$  in nanocrystalline  $\text{Co}_{1-x}\text{Zn}_x\text{Fe}_2\text{O}_4$  ferrite is obtained as  $\text{Zn}^{2+}$  ions concentration is around 0.3. Whereas, zinc ferrite is paramagnetic, coercivity  $H_c$  of nanocrystalline  $\text{Co}_{1-x}\text{Zn}_x\text{Fe}_2\text{O}_4$  ferrite gradually decreases with  $\text{Zn}^{2+}$  ions concentration.

#### 5. Conclusions

To summarize, we have prepared nanocrystalline  $\text{Co}_{1-x}\text{Zn}_x\text{Fe}_2\text{O}_4$  ferrite with a nanometer-scale grain size by using a spraying-coprecipitation process. The lattice parameters  $a$  of nanocrystalline  $\text{Co}_{1-x}\text{Zn}_x\text{Fe}_2\text{O}_4$  ferrites powder linearly increases with the  $\text{Zn}^{2+}$  ions concentration. The maximum specific saturation magnetization for nanocrystalline  $\text{Co}_{0.7}\text{Zn}_{0.3}\text{Fe}_2\text{O}_4$  ferrites reach up to  $83.4 \text{ A}\cdot\text{m}^2\cdot\text{kg}^{-1}$ . The coercivity  $H_c$  of samples decreased with the zinc ion concentration. This is ascribable to a change in the magnetic coupling between the sublattices of structure, which is due to the substitution of the  $\text{Co}^{2+}$  ions by  $\text{Zn}^{2+}$  ions.

#### Acknowledgements

This work was supported by National Nature Science Foundation of China (51174006), the Natural Science Foundation of High Education School of Anhui Province, China (KJ2010A095), Anhui Provincial Natural Science Foundation, China (1208085ME84) and The Project - sponsored by SRF for ROCS, SEM).

**References**

- [1] A. Thakur, P. Thakur, J. H. Hsu, *J. Appl. Phys.*, **111** (7), 305 (2012).
- [2] S. A. Morrison, C. L. Cahill, E. E. Carpenter, S. Calvin, R. Swaminathan, M. E. McHenry, V. G. Harris, *J. Appl. Phys.*, **95** 6392 (2004).
- [3] Z. Han, D. Li, X. G. Liu, D. Y. Geng, J. Li, Z. D. Zhang, *J. Phys. D: Appl. Phys.*, **42** 55008 (2009).
- [4] W. F. J. Fontijn, P. J. Van Der Zaag and R. Meselaar, *J. Appl. Phys.*, **83**(11), 6765 (1998).
- [5] K. J. Kim, H. S. Lee, M. H. Lee, S. H. Lee, *J. Appl. Phys.* **91**(12), 9974 (2002).
- [6] R. Rani, S. K. Sharma, K. R. Pirota, M. Knobel, S. Thakur, M. Singh, *Ceram. Intern.* **38**, 2389 (2012).
- [7] G. Vaidyanathan, S. Sendhilnathan, R. Arulmurugan, *J. Magn. Mater.*, **313**, 293 (2007).
- [8] L. Xiao, Fang Zheng, J. S. Liu, G. Z. Qiu, *Chin. J. Inorg. Chem.*, **22**(4), 729 (2006).
- [9] M. N. Palamaru, A. R. Iordan, C. D. Aruxandei, I. A. Gorodea, E. A. Perianu, I. Dumitru, M. Feder, O. F. Caltun, *J. Optoelectron. Adv. Mater.*, **10**(7), 1853 (2008).
- [10] A. M. Kumar, P. A. Rao, M. C. Varma, G. Choudary, K. H. Rao, *J Modern Phys.*, **2**, 1083 (2011).
- [11] G. V. Duong, N. Hanh, D. V. Linh, R. Groessinger, P. Weinberger, E. Schafler, M. Zehetbauer, *J Magn. Mater.*, **311**(1), 46 (2007).
- [12] L. Yin, Q. Tai, *Chin. Phys.* **16**(12), 3837 (2007).
- [13] B. D. Cullity. *Introduction to Magnetic Materials*. Addison-Wesley Reading, 1972.
- [14] E. P. Wohlfarth. *Ferromagnetic Materials*. North-Holland Publishing Co., 1980.
- [15] J. Smit, H. P. J. Wijn. *Ferrites*. Wiley, New York, 1959.
- [16] P. B. Rao, O. F. Caltun, *J. Optoelectron. Adv. Mater.*, **8**(3), 995 (2006).

---

\*Corresponding author: yinliu@aust.edu.cn